

Doping a moiré Mott insulator: A t - J model study of twisted cupratesXue-Yang Song , Ya-Hui Zhang, and Ashvin Vishwanath*Department of Physics, Harvard University, Cambridge, Massachusetts 02138, USA*

(Received 4 October 2021; revised 9 March 2022; accepted 20 April 2022; published 4 May 2022)

We theoretically explore twisted cuprate multilayers, a moiré material family where the individual layers are themselves strongly correlated. We study the twisted t - J model, using a slave-boson mean field treatment that is compatible with Mott physics at small doping. Furthermore, we incorporate the interlayer tunneling form-factor dictated by the symmetry of the Cu $d_{x^2-y^2}$ orbital. Including both these features leads to a phase diagram distinct from earlier weak-coupling treatments that predicted large gap spontaneous topological superconductors. Instead, we find that spontaneous time reversal (**T**) breaking occurs around twist angle of $\theta = 45^\circ$, but only in a narrow window. Moreover, a nearly gapless superconductor is obtained, whose spectroscopic features parallels that in monolayer cuprates, despite the broken time reversal and reflection symmetries. At smaller θ however, driving an interlayer current can lead to a gapped topological phase. The energy-phase relation of the interlayer Josephson junction displays notable double-Cooper-pair tunneling which dominates around 45° . The θ dependence of the Josephson critical current and the Shapiro steps are consistent with recent experiments. Utilizing the moiré structure as a probe of correlation physics, e.g., the pair density wave state, is discussed.

DOI: [10.1103/PhysRevB.105.L201102](https://doi.org/10.1103/PhysRevB.105.L201102)**I. INTRODUCTION**

Twisted heterostructures of graphene and transition metal dichalcogenides have attracted significant attention for displaying a series of interaction-driven phenomena such as superconductivity (SC) [1,2], integer and fractional Chern insulator phases [3–7] and as simulators of the Hubbard model [8–11]. Although the single layers tend to be weakly correlated, the twist structure reconstructs the electronic bands creating a versatile platform to study strongly interacting physics. A natural next step towards even richer phenomena are twisted bilayers where each layer itself is strongly correlated, e.g., twisted cuprate bilayers.

The recent fabrication of a high quality monolayer of $\text{Bi}_2\text{Sr}_2\text{CaCu}_2\text{O}_8$ ($\text{Bi}2212$) [11] finds similar critical temperature in monolayer and bulk cuprates, opening up the experimental study of cuprates as an essentially two-dimensional system. This also enables the experimental study of twisted cuprate bilayers, which has spurred pioneering theoretical proposals for two different realizations of topological SC in twisted cuprate bilayers [12,13]. Especially, Ref. [12] proposes a topological SC with time reversal(**T**) spontaneously broken when the twist angle $\theta \sim 45^\circ$, while Ref. [13] seeks to stabilize a similar state by tuning near a magic angle and establishing a superflow along the c axis. On experimental side, twisted cuprates have recently been fabricated and characterized [14,15]. Reference [15] reported a measurable second harmonic Josephson coupling at $\theta \approx 45^\circ$ based on the Shapiro step. However, so far there is no experimental signature of gap opening, spontaneous **T** breaking or topological SC.

In this Letter we study the twisted cuprate bilayers theoretically, augmenting earlier studies in three significant ways

(I) we introduce a microscopic twisted t - J model and solve it within the slave-boson mean-field approximation, which accounts for strong correlations. The d -wave pairing is obtained self-consistently, rather than put in by hand as in the Bardeen-Cooper-Schrieffer (BCS) framework [12]. (II) We incorporate the Mott physics in the slave-boson theory, known to be successful in capturing the d -wave SC in monolayers [16]. Here the effective interlayer tunneling is suppressed by a factor x , with $0 < x < 1$ the hole doping. Hence the method can smoothly crossover to the $x = 0$ limit (undoped Mott insulator) where interlayer tunneling is fully suppressed. (III) The interlayer tunneling should include a form factor $(\cos k_{x,t} - \cos k_{y,t})(\cos k_{x,b} - \cos k_{y,b})$ [17], where the momentum \mathbf{k}_t and \mathbf{k}_b are defined in the top and bottom layer, with the coordinate system fixed to the Cu-O bond of each layer. Such a form is important to consider since a uniform tunneling should vanish at $\theta = 45^\circ$ due to symmetries of the Cu $d_{x^2-y^2}$ orbitals.¹ The cosine form-factor suppresses tunneling around the nodal region. Therefore, the Dirac nodes remain almost gapless even if **T** is broken due to the pairing phase difference $\phi \neq 0, \pi$ between layers. Such momentum dependent tunneling and x factor make the window of θ with **T** breaking and gap significantly smaller than a previous study [12].

Our work has important implications for the ongoing experimental studies of twisted cuprate bilayers [15]. The critical Josephson current obtained demonstrates similar twist angle dependence as observed in experiment Ref. [15]. We

¹Strictly speaking, the oxygen p orbital is also involved in hole-doped cuprates, forming the Zhang-Rice singlet. However, a Wannier orbital is constructed with the same symmetry as the $d_{x^2-y^2}$ orbital

obtain the Shapiro steps at twist angle $\theta = 45.2^\circ$, consistent with those measured in Ref. [15], that supports the dominance of cooper pair cotunneling. Near 45° , we observe spontaneous **T** breaking as reported in Ref. [12]. However, due to additional ingredients in our treatment, we find no significant gap nor topological chiral modes. We note that there are two different manifestations of $d_{x^2-y^2}$ orbital symmetry in cuprates: one associated with the Cooper pair; the other one associated with the single electron orbital. It is known that the single Cooper pair tunneling is forbidden at $\theta = 45^\circ$ [12], which leads to **T** breaking. But it has not been noticed that the direct single electron tunneling is *also* forbidden for exactly the same reason, which interferes with realizing a robust topological superconductor at $\theta = 45^\circ$ in contrast to Ref. [12]. We calculate the polar Kerr effect [18,19] which can diagnose the **T** breaking.

Following Ref. [13], we find that topological SC can be induced by adding an interlayer supercurrent to give $\phi \neq 0$, despite that the magic angle is suppressed due to the x factor in the interlayer tunneling. This again highlights the importance of Mott physics in modeling twisted correlated bilayers.

II. MODEL FOR TWISTED DOUBLE-BILAYER Bi2212

We take the t - J model to describe a single cuprate layer on square lattice:

$$\mathcal{H}_{tJ} = -t \sum_{\langle ij \rangle} P c_{i,s}^\dagger c_{j,s} P + J \left(\mathbf{S}_i \cdot \mathbf{S}_j - \frac{1}{4} n_i n_j \right) + \mu \sum_i (n_i - 1), \quad (1)$$

where $s = \uparrow, \downarrow$; $n_i = \sum_s c_{i,s}^\dagger c_{i,s}$, $\mathbf{S} = \frac{1}{2} c_s^\dagger \boldsymbol{\sigma}_{ss'} c_{s'}$ and P projects out states with double/zero occupancy on any site for hole/electron doping, respectively. We take $t = 2J = 0.2$ eV in the calculation. The results stay qualitatively the same for $0.2t \lesssim J \lesssim 0.5t$ (Supplemental Material (SM) Fig. 2 [21]). A transformation $c_{is} \rightarrow c_{is}^\dagger$ relates electron to hole doping cases, with the sign of t, μ changed.

Motivated by experiment [14,15] we consider twisted *double* bilayers, and add an index $p = t_1, t_2, b_1, b_2$ denoting operators in the top first, top second, bottom first and bottom second layers, shown in Fig. 1. Layers t_2 and b_1 are twisted with a relative angle θ . Each layer is hence defined as top (bottom) bilayers. The full Hamiltonian should include interlayer tunneling with strength t_z as

$$\begin{aligned} \mathcal{H}_{tbsc} = & \sum_{i=1,2} \mathcal{H}_{tJ,ti} + \mathcal{H}_{tJ,bi} - t_z \sum_{ij} F_{tb}(\mathbf{r}_{ij}) c_{i,t2}^\dagger c_{j,b1} \\ & - t_o \sum_{ij,p=t,b} F_p(\mathbf{r}_{ij}) c_{i,p1}^\dagger c_{j,p2} + \text{H.c.}, \end{aligned} \quad (2)$$

where the second line describes tunneling within unit cell, in Fourier space as [20] $F_p(\mathbf{k}) = (\cos k_{x,p} - \cos k_{y,p})^2/4 + 0.4$, \mathbf{k} in the original Brillouin zone.

Interlayer tunneling between d orbitals consists of 2 processes, plotted in Fig. 1(a): The first one is mediated by Cu s orbital through a three-step virtual process. In real space the step (I) and (III) are from intralayer nearest neighbor hopping $c_i^\dagger s_{i\pm\hat{x}} - c_i^\dagger s_{i\pm\hat{y}} + \text{H.c.}$, where s_i^\dagger create electron at Cu s orbital, which is at higher energy and should be inte-

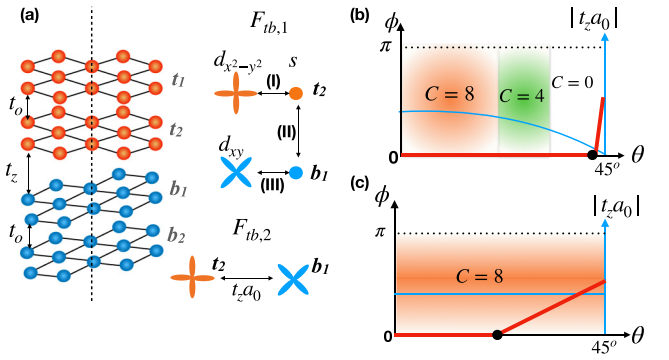


FIG. 1. (a) A schematic plot of the twisted 4 CuO layers. The sites within the top, bottom bilayers are perfectly aligned. There is an hopping within unit cell with strength t_o and interlayer hopping with strength t_z . Tunneling across the twist consists of two processes: $F_{tb,1}$ is a three step tunneling process mediated by s orbital of Cu and $F_{tb,2}$ describes a direct tunneling between d orbitals of Cu. The *single electron* orbital $d_{x^2-y^2}$ is rotated relatively between layers, constraining interlayer tunneling $F_{tb}(\mathbf{r})$. (b), (c) The schematic phase diagrams of twisted cuprates with physical reflection-symmetric tunneling (b) or artificial reflection-violating (c) tunneling. The red curve depicts the optimal pairing difference ϕ with the onset of spontaneous **T** breaking marked by black dots. Blue curves are the uniform tunneling strength that breaks R_{xy} at 45° in (c). (b) considers both cos form and uniform tunneling which vanishes at $\theta = 45^\circ$ as required by reflection symmetry. It is clear that the window of **T** breaking is much narrower ($\delta\theta \sim 4^\circ$) than (c) ($\delta\theta > 30^\circ$). This implies that one is always in the weak nodal tunneling regime when **T** breaking occurs. Chern numbers are shown for different θ . Other Chern numbers, e.g., $C = 2, 6$ can be realized with different tunneling strength. (c) considers only uniform tunneling (actual data of $\phi(\theta)$ in the SM Fig. 4 [21]), comparable to Ref. [12].

grated. In momentum space these two steps contribute a factor $(\cos k_{x,t} - \cos k_{y,t})(\cos k_{x,b} - \cos k_{y,b})$. Step II is from tunneling of the s orbitals.

The second one is a direct, uniform tunneling controlled by a_0 [20]. Both tunnelings involve exponentially decay amplitude for interlayer hopping encoded by $g_s(i_{t2}, j_{b1}) = e^{-(l_{ij}-l_d)/\rho}$. Here $l_{ij} = |i_{t2} - j_{b1}|$ and $l_d \approx 2a_{Cu}$ ($a_{Cu} \approx 0.3$ nm the lattice constant of CuO plane) is the distance between layers, and $\rho \approx 0.5a_{Cu}$ is a tunneling parameter. The two processes read in real space [21]

$$\begin{aligned} F_{tb,1}(\mathbf{r}_{ij}) = & \frac{1}{2} \sum_{\hat{h}'=x',y'} \xi_{\hat{h}} \xi_{\hat{h}'} g_s(r_{i\pm\hat{h},j\pm\hat{h}'}), \\ \xi_{\hat{x}} = & 1, \quad \xi_{\hat{y}} = -1, \quad F_{tb,2}(\mathbf{r}_{ij}) = a_0 g_s(i_{t2}, j_{b1}). \end{aligned} \quad (3)$$

From reflection R_{xy} and based on Cu $d_{x^2-y^2}$ orbital symmetries, one deduces [21]

$$a_0(\theta) = -a_0(90^\circ - \theta), \quad a_0(45^\circ) = 0. \quad (4)$$

At 45° a reflection that exchanges x, y coordinates in the top layer will change the sign of its d orbital wave function, while for the bottom layer the reflection sends $x \rightarrow -x$ and its d orbital wave function unchanged. Hence the direct hopping between d orbitals vanishes due to the different transform under R_{xy} . This form is not a minor addition to

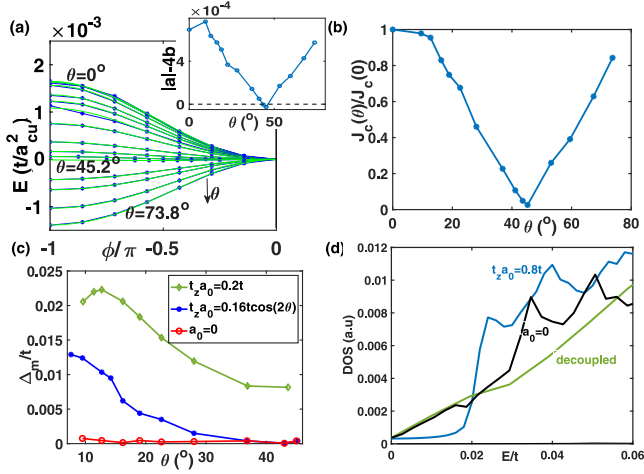


FIG. 2. Data at $x = 0.2$, $t_z = 0.1t$. (a) The mean-field energy E vs pairing phase difference ϕ for various θ , at $a_0 = 0$. The inset plots $|a| - 4b$ from curve fits $E = -a(\theta)\cos(\phi) + b(\theta)\cos(2\phi)$, which, when negative, indicates energy minima at nontrivial $\phi \neq 0, \pi$. At $\theta = 43.6, 45.2^\circ$ we have an energy minimum at nontrivial $\phi \approx 0.16\pi, 0.64\pi$, respectively. (b) Critical Josephson current density normalized by the untwisted value at $a_0 = 0$. $J_c(45.2^\circ) = 2000$ kA/cm², while $J_c(0^\circ) = 8 \times 10^4$ kA/cm². (c) The maximal gap Δ_m , obtained by varying ϕ at fixed θ , for uniform tunneling, realistic mixed tunneling (blue) and only cos form tunneling ($a_0 = 0$), respectively. (d) The density of states at $\theta = 43.6^\circ$ for large uniform tunneling (blue) with a gap $\sim 4\%t$, decoupled layers (green) and cos form tunneling (black) with a vanishing gap $< 0.001t$. Green and black curves are indistinguishable at low energy. So scanning tunneling microscopy (STM) would not show a qualitative difference between twisted and decoupled cuprate bilayers.

Ref. [12]. Single-particle orbitals in cuprates are classified into irreducible representations of R_{xy} . The active d orbitals we consider are odd under R_{xy} , while Ref. [12] implicitly assumes s orbitals dominate the tunneling. Vanishing of a_0 close to 45° qualitatively modifies the phase diagram [Fig. 1(b)] for twisted cuprates, compared with Fig. 1(c) which falsely assumes identical a_0 for all θ . Figure 1(b) displays a much narrower θ window of spontaneous \mathbf{T} breaking with nontrivial ϕ (red line) and the change of band topology to trivial close to 45° , indicated by the Chern number.

III. SLAVE-BOSON MEAN-FIELD THEORY

To decouple the Hamiltonian we adopt a parton decomposition for electron operators, $c_{i,s} = b_i^\dagger f_{i,s}$, with fermionic spinons f_s and bosonic holons b . There is a gauge constraint $\sum_s f_{i,s}^\dagger f_{i,s} + b_i^\dagger b_i = 1$ to exclude double occupancy, and the electron number reads $n_i = 1 - b_i^\dagger b_i = 1 - x_i$.

Upon doping with a fraction x of holes, the condition becomes $\sum_i b_i^\dagger b_i = Nx$ with N being the number of sites. The holons will condense ($x > 0$) to $\langle b_i \rangle = \sqrt{x_i}$. Substituting the condensed holon operator into the t - J Hamiltonian Eq. (2), and further decoupling $\mathbf{S}_i \cdot \mathbf{S}_j$ [22], one gets (assuming spin

rotation invariance)

$$\begin{aligned} \mathcal{H}_{\text{MF}} = & \sum_{p=t(b)} \left\{ - \sum_{\langle ij \rangle, s} \left[\left(t \sqrt{x_{ip} x_{jp}} + \frac{3J}{8} \chi_{ij,p}^* \right) f_{isp}^\dagger f_{isp} + \text{H.c.} \right] \right. \\ & - \frac{3J}{8} \sum_{\langle ij \rangle, ss'} [\Delta_{ij,p}^* f_{is,p} f_{js',p} \epsilon_{ss'} + \text{H.c.}] + \mu_p \sum_i n_{ip} \left. \right\} \\ & - t_z \sum_{ij,x} F_{tb}(\mathbf{r}_{ij}) e^{-(l_{ij}-l_d)/\rho} \sqrt{x_{i,t2} x_{j,b1}} f_{is,t2}^\dagger f_{js,b1} \\ & - t_o \sum_{ij,p=t,b} F_p(\mathbf{r}_{ij}) \sqrt{x_{i,p1} x_{j,p2}} f_{i,p1}^\dagger f_{j,p2} + \text{H.c.}, \quad (5) \end{aligned}$$

where we mainly consider the mean-field order parameters for hopping $\chi_{ij} = \sum_s \langle f_{is}^\dagger f_{js} \rangle$, pairing $\Delta_{ij} = \sum_{ss'} \epsilon_{ss'} \langle f_{is} f_{js'} \rangle$. The interlayer tunneling $F_{tb} = F_{tb,1} + F_{tb,2}$ consists of two processes in Eq. (3).

The parton construction naturally incorporates the Mott insulating state at vanishing doping x , since the system will enter a staggered flux state that describes an antiferromagnet with vanishing tunneling.

For a mean-field treatment, we start with unbiased random pairing ansatz, and converge to a d -wave pairing ansatz, i.e., $\Delta_{i,i+\hat{x},t(b)} = -\Delta_{i,i+\hat{y},t(b)} = \delta_{i,t(b)} e^{i\phi_{i(b)}}$. In this way we reach a mean-field minimum of the free energy, with the pairing phase difference $\phi = \phi_t - \phi_b$. We can also explicitly choose the ansatz with an arbitrary ϕ and calculate the energy $E(\phi)$. We fix the doping x in each simulation and the chemical potential μ is adjusted in each iteration to keep x unchanged [21]. Our slave particle mean-field theory includes a large number $\sim 10^2 - 10^3$ parameters due to the moiré unit cell size. The calculation nevertheless converges to a d -wave pairing state. While other work including Ref. [12] heuristically adds an interaction favoring d -wave pairing, here the pairing symmetry and quantitative aspects naturally emerge from the antiferromagnetic J as the only input.

IV. CRITICAL JOSEPHSON CURRENT

From the energy-phase relation in Fig. 2(a),² one could extract critical Josephson current density by $J_c = \frac{2e}{\hbar A} \max_\phi \left(\frac{dE}{d\phi} \right)$ (A the system area) as Fig. 2(b). The curve agrees qualitatively with Ref. [15]. The decrease in J_c as θ moves toward 45° implies dominant d -wave pairing in cuprates.

On the absolute value of J_c , Ref [14] reports $J_c \approx 100$ A/cm² at $\theta = 45^\circ$, doping $x = 0.1$. Reference [15] reports a smaller $J_c(45^\circ) \approx 40 - 120$ A/cm². Numerically we find $J_c(45^\circ) \approx 50$ kA/cm² at $t_z = 0.05t$, $x = 0.1$, 500 times larger than experiment. This reduction in critical current is puzzling, and similar discrepancies have been reported for untwisted cuprates [23]. We conjecture it is the vortex

²The energy variation upon varying ϕ comes mainly from interlayer tunneling terms and we calculate energy only from interlayer tunneling terms hereafter.

dynamics or disorder effects, rather than t - J physics, that determines J_c .

V. $\theta \sim 45^\circ$: CHIRAL NONTOPOLOGICAL SC AND ANOMALOUS HALL EFFECTS

The system energetically favors a nonzero ϕ and spontaneously breaks \mathbf{T} symmetry close to 45° . Figure 2(a) inset shows the fitting parameters a, b in the energy-phase relation, $E(\phi) = -a \cos \phi + b \cos 2\phi + \text{const}$. At $\theta = 43.6^\circ, 45.2^\circ$, we have $4|b| > |a|$ and an optimal $\phi \approx 0.16\pi, 0.64\pi$, respectively. While for other angles, optimal $\phi = 0, \pi$ for $\theta < 41.2^\circ, > 48.8^\circ$, respectively.

Spontaneous \mathbf{T} breaking from $\phi \neq 0$ has been pointed out previously [12]. However, the chiral (\mathbf{T} breaking) SC here is qualitatively different. First, due to the x factor appearing in tunneling from the slave bosons, the window of twist angle with $\phi \neq 0$ is significantly smaller in our calculation, i.e., $43^\circ \lesssim \theta \lesssim 47^\circ$, plotted in Fig. 1(b). Moreover, the chiral SC shows a very small gap, because the form factor $\cos k_x - \cos k_y$ is suppressed at nodal region ($k_x = k_y$). Thus the gap [red line in Fig. 2(c)] is suppressed even if ϕ is large. A significant uniform tunneling, imposed by hand, will open a larger gap [green line in Fig. 2(c)]. The DoS shows qualitative differences at small energy between cases with or without uniform tunneling in Fig. 2(d): DoS is V shaped (black, vanishing gap) with only cos form tunneling, similar to that of decoupled monolayers (green). In contrast, the DoS has a vanishing flat segment (blue) at low energy corresponding to the gap opened by large uniform tunneling. We use a four-band continuum model in the SM [21] to explain why cos form tunneling opens a much smaller gap than uniform tunneling.

Also, we find that the Chern number is 0, both for twisted double-bilayer and twisted bilayer Bi2212 (i.e., retaining only layers t_2, b_1 shown in SM Fig. [21]). Therefore a topological SC is *absent* close to 45° , in contrast to Ref. [12]. If we ignore the form factor and take uniform tunneling, we recovered results in Ref. [12] qualitatively, e.g., the gap, Chern number etc. [21] Unfortunately such an s-wave interlayer tunneling vanishes by symmetry at $\theta = 45^\circ$.

The DoS in the chiral SC is still V shaped [Fig. 2(d)] in the experimentally relevant energy scale. Therefore it is not possible to detect the \mathbf{T} breaking using electron spectroscopy such as STM or angle-resolved photoemission spectroscopy. We note that finite Hall conductivity $\sigma_h(\omega)$ signals \mathbf{T} breaking, plotted in Fig 3(a,b), measurable in Terahertz spectroscopy [21,24–27]. From Fig. 3(b) we estimate a Kerr angle $\theta_K \sim 1 \mu\text{rad}$ at $\omega \sim 30 \text{ meV}$ for the polar Kerr effect [19] at 43.6° . The nonzero σ_h for a range of x, t_z in Fig. 3(a) attests to the stability of \mathbf{T} breaking when varying doping (chemical potential) or tunneling. We also find a nonzero c -axis magnetization, plotted in SM 3 [21]. Hence the chiral state at 45° is featureless in STM, but \mathbf{T} breaking has distinct signatures in Hall conductivity, etc.

VI. TOPOLOGICAL SC AND FLAT BAND AT SMALL θ

At small θ , we take $t_z a_0 = 0.16t$ as the uniform tunneling and find \mathbf{T} is preserved. If one adds by hand an interlayer supercurrent (to model a uniform current state along the c axis)

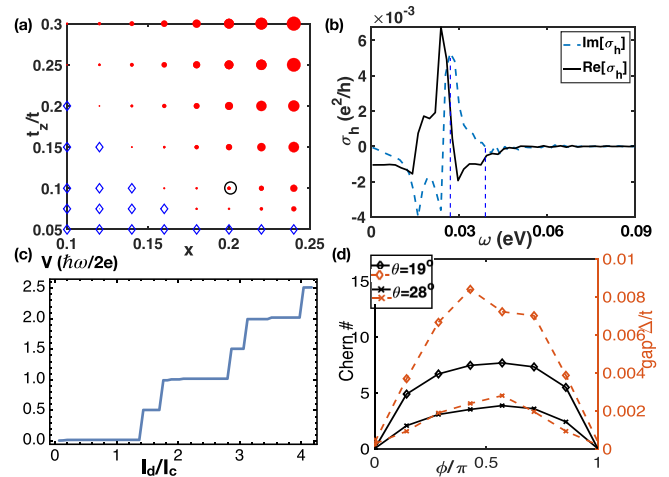


FIG. 3. Data for $t_z = 0.1t, x = 0.2$. (a)–(c) take $\theta = 43.6^\circ, a_0 = 0$. (a) The real part of Hall conductivity $\text{Re}[\sigma_h(\omega \rightarrow 0)]$ (indicated by the red disk size) as x and t_z vary, signaling \mathbf{T} breaking. The blue diamonds denote absence of \mathbf{T} breaking, i.e., $\sigma_h(\omega) = 0$. (b) Real and Imaginary parts of $\sigma_h(\omega)$ at one particular parameter set $\phi = 3\pi/16$ (circled in (a)). The edge above which σ_h tends to 0 at $\omega/t \approx 0.2$ corresponds to the maximal gap around Fermi surface (SM Fig. 6 [21]) in untwisted cuprates. (c) The Shapiro step measured in resistively shunted Josephson junction with DC current I_d and an AC current I_{rf} with frequency ω . The time-averaged voltage displays steps as I_d is increased, in particular the half steps indicate a second harmonic term in energy-phase relation. Parameters $\theta = 45.2^\circ, b = -1.3a$, with $I_{rf} = 1.25I_c, \omega = 0.5I_c/e$ (I_c the critical Josephson current). (d) The Chern number (black) and gap (orange) upon varying ϕ for two relatively small twist angles with mixed tunneling and $t_z a_0 = 0.16t, 0.12t$ for $\theta = 19^\circ, 28^\circ$, respectively.

by fixing $\phi \neq 0, \pi$, topological SC emerges, indicated by Chern numbers plotted in Fig. 3(d).³ This confirmed predictions about topological SC at small θ in Ref. [13], and goes beyond small angle approximation to show that topological SC occurs for larger θ as well. The gap for the topological SC is shown in Fig. 3(d).

To locate the flat band, since the x factor suppresses tunneling, we expect the magic angle is suppressed from $\theta_{MA} \approx \frac{T_z}{2v_F Q}$, where T_z is effective tunneling strength and Q the node momentum. Indeed in Fig. 2(c), the maximal possible gap Δ_m (blue curve for mixed tunneling) upon varying ϕ keeps increasing as twist angle θ is reduced to 9.7° , indicating flat band may exist for $\theta < 9.7^\circ$, if at all. For uniform tunneling only, Δ_m reaches the maximum at $\theta \approx 13^\circ$. In Ref. [13], a magic angle around 13.8° is predicted for Bi2212 from a BCS model analysis.

For $\theta \sim 45^\circ$, a relatively flat portion near *top* of the lowest conduction band is found (SM 7 [21]). This could result in an enhanced signal in optical measurements.

³Chern number for $\theta = 19^\circ, 28^\circ$ reaches the maximal value of 7.7, 3.8, the non-quantization is due to numerical precision and is assigned to have $C = 8, 4$ respectively.

VII. MOIRÉ AS A PROBE OF CORRELATION PHYSICS

We propose to detect the pair-density-wave (PDW) [28–35] SC in twisted cuprate bilayers using the interlayer pair tunneling. A bias is applied to give different doping in the two layers, making it possible to have $T > T_c^a, T < T_c^b$, where T_c^a, T_c^b are the critical temperature for the d -wave SC of the two layers. The bottom layer is in the SC phase, while the top layer is in the pseudogap (PG) phase. We have a PG-SC junction instead of the SC-SC junction. At $\theta \approx 7.18^\circ$, the moiré superlattice naturally provides a momentum $\mathbf{G}_M \approx (\frac{2\pi}{8a}, 0)$, close to the momentum of the PDW expected in the PG regime [34,35]. Then it is possible to detect the PDW fluctuation susceptibility $\text{Im}\chi(\omega, q)$ using interlayer pair tunneling following Refs. [21,36,37].

VIII. CONCLUSIONS

Through a self-consistent mean-field study of a t - J model for twisted double-bilayer cuprates, we find a \mathbf{T} breaking

but nontopological SC at a twist angle around 45° . Our conclusions rely on incorporating Mott physics and a form factor in the tunneling, crucial in the modeling of twisted cuprates. With microscopic calculations, we provide twist angle dependence of the critical Josephson current, in qualitative agreement with the recent experiment [15]. Finite temperature extensions and the interplay of correlation phenomena within the moiré structure will be interesting to explore further.

Note added. During the finalization of the manuscript, we became aware of two preprints [38,39] which also study the twisted cuprate bilayer and discuss the critical Josephson current.

ACKNOWLEDGMENTS

We thank P. Kim, X. Cui, and M. Randeria for discussions. This research was funded by a Simons Investigator award (A.V.), the Simons Collaboration on Ultra-Quantum Matter, which is a grant from the Simons Foundation (651440, A.V.), and a 2019 grant from the Harvard Quantum Initiative Seed Funding program.

-
- [1] Y. Cao, V. Fatemi, S. Fang, K. Watanabe, T. Taniguchi, E. Kaxiras, and P. Jarillo-Herrero, Unconventional superconductivity in magic-angle graphene superlattices, *Nature (London)* **556**, 43 (2018).
- [2] Y. Cao, V. Fatemi, A. Demir, S. Fang, S. L. Tomarken, J. Y. Luo, J. D. Sanchez-Yamagishi, K. Watanabe, T. Taniguchi, E. Kaxiras, R. C. Ashoori, and P. Jarillo-Herrero, Correlated insulator behaviour at half-filling in magic-angle graphene superlattices, *Nature (London)* **556**, 80 (2018).
- [3] A. L. Sharpe, E. J. Fox, A. W. Barnard, J. Finney, K. Watanabe, T. Taniguchi, M. A. Kastner, and D. Goldhaber-Gordon, Emergent ferromagnetism near three-quarters filling in twisted bilayer graphene, *Science* **365**, 605 (2019).
- [4] M. Yankowitz, S. Chen, H. Polshyn, Y. Zhang, K. Watanabe, T. Taniguchi, D. Graf, A. F. Young, and C. R. Dean, Tuning superconductivity in twisted bilayer graphene, *Science* **363**, 1059 (2019).
- [5] X. Lu, P. Stepanov, W. Yang, M. Xie, M. A. Aamir, I. Das, C. Urgell, K. Watanabe, T. Taniguchi, G. Zhang, A. Bachtold, A. H. MacDonald, and D. K. Efetov, Superconductors, orbital magnets and correlated states in magic-angle bilayer graphene, *Nature (London)* **574**, 653 (2019).
- [6] Y. Xie, A. T. Pierce, J. M. Park, D. E. Parker, E. Khalaf, P. Ledwith, Y. Cao, S. H. Lee, S. Chen, P. R. Forrester, K. Watanabe, T. Taniguchi, A. Vishwanath, P. Jarillo-Herrero, and A. Yacoby, Fractional Chern insulators in magic-angle twisted bilayer graphene, *Nature* **600**, 439 (2021).
- [7] T. Li, S. Jiang, B. Shen, Y. Zhang, L. Li, T. Devakul, K. Watanabe, T. Taniguchi, L. Fu, J. Shan, and K. F. Mak, Quantum anomalous Hall effect from intertwined moiré bands, *Nature* **600**, 641 (2021).
- [8] F. Wu, T. Lovorn, E. Tutuc, and A. H. MacDonald, Hubbard Model Physics in Transition Metal Dichalcogenide Moiré Bands, *Phys. Rev. Lett.* **121**, 026402 (2018).
- [9] Y. Tang, L. Li, T. Li, Y. Xu, S. Liu, K. Barmak, K. Watanabe, T. Taniguchi, A. H. MacDonald, J. Shan, and K. F. Mak, Simulation of Hubbard model physics in WSe_2/WS_2 moiré superlattices, *Nature* **579**, 353 (2020).
- [10] E. C. Regan, D. Wang, C. Jin, M. I. Bakti Utama, B. Gao, X. Wei, S. Zhao, W. Zhao, Z. Zhang, K. Yumigeta, M. Blei, J. D. Carlström, K. Watanabe, T. Taniguchi, S. Tongay, M. Crommie, A. Zettl, and F. Wang, Mott and generalized Wigner crystal states in WSe_2/WS_2 moiré superlattices, *Nature (London)* **579**, 359 (2020).
- [11] L. Wang, E.-M. Shih, A. Ghiotto, L. Xian, D. A. Rhodes, C. Tan, M. Claassen, D. M. Kennes, Y. Bai, B. Kim *et al.*, Correlated electronic phases in twisted bilayer transition metal dichalcogenides, *Nat. Mater.* **19**, 861 (2020).
- [12] O. Can, T. Tummuru, R. P. Day, I. Elfimov, A. Damascelli, and M. Franz, High-temperature topological superconductivity in twisted double-layer copper oxides, *Nat. Phys.* **17**, 519 (2021).
- [13] P. A. Volkov, J. H. Wilson, and J. H. Pixley, Magic angles and current-induced topology in twisted nodal superconductors (2020), [arXiv:2012.07860](https://arxiv.org/abs/2012.07860) [cond-mat.supr-con].
- [14] Y. Zhu, M. Liao, Q. Zhang, H.-Y. Xie, F. Meng, Y. Liu, Z. Bai, S. Ji, J. Zhang, K. Jiang, R. Zhong, J. Schneeloch, G. Gu, L. Gu, X. Ma, D. Zhang, and Q.-K. Xue, Presence of s -Wave Pairing in Josephson Junctions Made of Twisted Ultrathin $\text{Bi}_2\text{Sr}_2\text{CaCu}_2\text{O}_{8+x}$ Flakes, *Phys. Rev. X* **11**, 031011 (2021).
- [15] S. Y. F. Zhao, N. Poccia, X. Cui, P. A. Volkov, H. Yoo, R. Engelke, Y. Ronen, R. Zhong, G. Gu, S. Plugge, T. Tummuru, M. Franz, J. H. Pixley, and P. Kim, Emergent interfacial superconductivity between twisted cuprate superconductors (2021), [arXiv:2108.13455](https://arxiv.org/abs/2108.13455) [cond-mat.supr-con].
- [16] P. A. Lee, N. Nagaosa, and X.-G. Wen, Doping a mott insulator: Physics of high-temperature superconductivity, *Rev. Mod. Phys.* **78**, 17 (2006).
- [17] O. K. Andersen, A. I. Liechtenstein, O. Jepsen, and F. Paulsen, LDA energy bands, low-energy Hamiltonians, t' , t'' , $t_\perp(k)$, and j_\perp , *J. Phys. Chem. Solids* **56**, 1573 (1995).

- [18] A. Kapitulnik, J. Xia, E. Schemm, and A. Palevski, Polar kerr effect as probe for time-reversal symmetry breaking in unconventional superconductors, *New J. Phys.* **11**, 055060 (2009).
- [19] O. Can, X.-X. Zhang, C. Kallin, and M. Franz, Probing Time Reversal Symmetry Breaking Topological Superconductivity in Twisted Double Layer Copper Oxides with Polar Kerr Effect, *Phys. Rev. Lett.* **127**, 157001 (2021).
- [20] R. S. Markiewicz, S. Sahrakorpi, M. Lindroos, H. Lin, and A. Bansil, One-band tight-binding model parametrization of the high- T_c cuprates including the effect of k_z dispersion, *Phys. Rev. B* **72**, 054519(R) (2005).
- [21] See Supplemental Material at <http://link.aps.org/supplemental/10.1103/PhysRevB.105.L201102> for details on tunneling forms, symmetries, parameter choices from band structures of Bi2212, numerical procedure to solve t - J model, Hall conductivity, comparison with BCS calculation results, detection of PDW fluctuations, and Supplemental figures.
- [22] Q.-H. Wang, D.-H. Lee, and P. A. Lee, Doped t - J model on a triangular lattice: Possible application to $\text{Na}_x\text{CoO}_2 \cdot y\text{H}_2\text{O}$ and $\text{Na}_{1-x}\text{TiO}_2$, *Phys. Rev. B* **69**, 092504 (2004).
- [23] D. E. Sheehy, T. P. Davis, and M. Franz, Unified theory of the ab plane and c axis penetration depths of underdoped cuprates, *Phys. Rev. B* **70**, 054510 (2004).
- [24] C. Kallin and J. Berlinsky, Chiral superconductors, *Rep. Prog. Phys.* **79**, 054502 (2016).
- [25] J.-L. Zhang, Y. Li, W. Huang, and F.-C. Zhang, Hidden anomalous Hall effect in Sr_2RuO_4 with chiral superconductivity dominated by the Ru d_{xy} orbital, *Phys. Rev. B* **102**, 180509 (2020).
- [26] M. D. E. Denys and P. M. R. Brydon, Origin of the anomalous Hall effect in two-band chiral superconductors, *Phys. Rev. B* **103**, 094503 (2021).
- [27] J. Hwang, T. Timusk, and G. D. Gu, Doping dependent optical properties of $\text{Bi}_2\text{Sr}_2\text{CaCu}_2\text{O}_{8+\delta}$, *J. Phys.: Condens. Matter* **19**, 125208 (2007).
- [28] M. Raczkowski, M. Capello, D. Poilblanc, R. Frésard, and A. M. Oleś, Unidirectional d -wave superconducting domains in the two-dimensional t - j model, *Phys. Rev. B* **76**, 140505(R) (2007).
- [29] D. F. Agterberg, J. C. S. Davis, S. D. Edkins, E. Fradkin, D. J. Van Harlingen, S. A. Kivelson, P. A. Lee, L. Radzihovsky, J. M. Tranquada, and Y. Wang, The physics of pair-density waves: cuprate superconductors and beyond, *Annu. Rev. Condens. Matter Phys.* **11**, 231 (2020).
- [30] A. Himeda, T. Kato, and M. Ogata, Stripe States with Spatially Oscillating d -Wave Superconductivity in the Two-Dimensional t - t' - j Model, *Phys. Rev. Lett.* **88**, 117001 (2002).
- [31] E. Berg, E. Fradkin, E.-A. Kim, S. A. Kivelson, V. Oganesyan, J. M. Tranquada, and S. C. Zhang, Dynamical Layer Decoupling in a Stripe-Ordered High- T_c Superconductor, *Phys. Rev. Lett.* **99**, 127003 (2007).
- [32] E. Berg, E. Fradkin, S. A. Kivelson, and J. M. Tranquada, Striped superconductors: How spin, charge and superconducting orders intertwine in the cuprates, *New J. Phys.* **11**, 115004 (2009).
- [33] E. Fradkin, S. A. Kivelson, and J. M. Tranquada, Colloquium: Theory of intertwined orders in high temperature superconductors, *Rev. Mod. Phys.* **87**, 457 (2015).
- [34] P. A. Lee, Amperean Pairing and the Pseudogap Phase of Cuprate Superconductors, *Phys. Rev. X* **4**, 031017 (2014).
- [35] S. D. Edkins, A. Kostin, K. Fujita, A. P. Mackenzie, H. Eisaki, S. Uchida, S. Sachdev, M. J. Lawler, E.-A. Kim, J. C. S. Davis *et al.*, Magnetic field-induced pair density wave state in the cuprate vortex halo, *Science* **364**, 976 (2019).
- [36] D. J. Scalapino, Pair Tunneling as a Probe of Fluctuations in Superconductors, *Phys. Rev. Lett.* **24**, 1052 (1970).
- [37] P. A. Lee, Proposal to measure the pair field correlator of a fluctuating pair density wave, *Phys. Rev. B* **99**, 035132 (2019).
- [38] P. A. Volkov, S. Y. F. Zhao, N. Poccia, X. Cui, P. Kim, and J. H. Pixley, Josephson effects in twisted nodal superconductors (2021), [arXiv:2108.13456](https://arxiv.org/abs/2108.13456) [cond-mat.supr-con].
- [39] T. Tummuru, S. Plugge, and M. Franz, Josephson effects in twisted cuprate bilayers, *Phys. Rev. B* **105**, 064501 (2022).